AD-A063 652 TEXAS A AND M UNIV COLLEGE STATION DEPT OF PHYSICS F/G 4/1
RADIATIVE TRANSFER IN AN ATMOSPHERE-OCEAN SYSTEM: A MATRIX OPER--ETC(U)
JUL 78 G W KATTAWAR, T J HUMPHREYS, G N PLASS N00014-75-C-0537

UNCLASSIFIED 13 NL

| OF |
AD
A063 652

END
DATE
FILMED
3--79
DDC

Radiative Transfer in an Atmosphere-Ocean System: A Matrix Operator Approach

By

George W. Kattawar, Terry J. Humphreys, Gilbert N. Plass

Report No. 13

28p.

The research described in this report was funded by The Ocean Science and Technology Division of the Office of Naval Research

Contract N00014-75-C-0537

Department of Physics
Texas A&M University
College Station, Texas 77843

27 July 1978

This report has been submitted to the Society of Photo-Optical Instrumentation Engineers.

Radiative Transfer in an Atmosphere-Ocean System: A Matrix Operator Approach

George W. Kattawar, Terry J. Humphreys, and Gilbert N. Plass

ABSTRACT

It is the purpose of this paper to demonstrate how the matrix operator method can be effectively implemented to couple the radiation fields of the atmophere and ocean. Azimuthally averaged radiances and irradiances are presented as a function of optical depth for a conservative Rayleigh scattering medium of total optical thickness τ_{max} = 1000 with a dielectric interface placed at optical depths of 0.01, 0.1, 1.0, and 10.0, and for various solar incident angles.

INTRODUCTION

In order for us to understand the effect of changes in optical properties of either the atmosphere or ocean on the radiation field, we must be able to perform accurate radiative transfer calculations for this coupled system. It is important for researchers in the remote sensing area to know not only what regions of the spectrum are affected but to what degree they are affected by known changes in the optical properties of the medium. One area of extreme importance is the remote sensing of phytoplankton in a body of water since these organisms essentially determine the effective productivity. In addition to the radiation in vitro for remote sensing purposes one is also interested in the radiation in situ for biological purposes since the irradiance is an important factor in photosynthesis.

To perform a radiative transfer calculation at any particular frequency, we need only two quantities, namely $\beta(\Theta)$ (the volume scattering function in units of m^{-1} sr^{-1}) and c (the attenuation coefficient in units of m^{-1}). Now if the medium is inhomogeneous, then we must specify these quantities at each depth within the medium. Other useful quantities derivable from these two are:

The authors are with the Texas A&M University, Physics Department, College Station, Texas 77843.

$$b \text{ (scattering coefficient)} = 2\pi_0 \int^{\pi} \beta(\Theta) \sin\Theta \, d\Theta, \tag{1}$$

$$P(\Theta) \text{ (phase function)} = \beta(\Theta)/b, \tag{2}$$

where

$$2\pi_0 \int^{\pi} P(\Theta) \sin\Theta \, d\Theta = 1, \tag{3}$$

$$a \text{ (absorption coefficient)} = c - b \tag{4}$$

$$\omega_0 \text{ (single scattering albedo)} = b/c, \tag{5}$$

and

$$\tau \text{ (optical depth between layers at } z_1 \text{ and } z_2) = \int_{z_1}^{z_2} c \, dz. \tag{6}$$

It should be emphasized that all of the optical parameters as given are for all constituents within the sample being considered.

If we let $I(\tau,\mu,\phi)$ denote the radiance then the equation of transfer assumes the following form

$$\left(\mu \frac{d}{d\tau} + 1\right) I(\tau,\mu,\phi) = \omega_0 \int_{-1}^{1} \int_{0}^{2\pi} P(\tau,\mu,\phi;\mu';\phi') \, I(\tau;\mu;\phi') d\mu' d\phi' \tag{7}$$

where we have adopted the convention that $\mu > 0$ denotes downward moving radiation and $\mu < 0$ denotes upward moving radiation. It is the purpose of this article to demonstrate that quite accurate solutions to this equation can be obtained by the matrix operator technique subject to various boundary conditions.

BASIC THEORY

The historical development of the matrix operator theory can be found in Plass, et.al.[1], and we will not go into the details of discretization

or Fourier decomposition. The fundamental problem arises when we couple the atmosphere to the ocean through a dielectric interface. Let us assume that we have a discrete set of N cosines of the polar angle $0 < \theta \leq \pi/2$ for the ocean such that $\mu_i = \cos \theta_i > 0$. Similarly we will have a set of points $\mu_i = -\cos \theta_i < 0$ which will label the upper hemisphere (see Fig. 1). Out of the set of N points for the ocean only M of them can be mapped into the atmosphere i.e., those for which $\mu_i > \cos \theta_c$ where θ_c is the critical angle defined by $\sin \theta_c = 1/n$ where n is the refractive index of water. The remaining N-M points are restricted to the ocean and cannot be mapped into the atmosphere. These points specify the region of total internal reflection. The relationship connecting α to θ is simply Snell's law, namely

$$\sin \alpha_i = n \sin \theta_i \tag{8}$$

or

$$\xi_i = (1 - (1 - \mu_i^2)n^2)^{1/2} \tag{9}$$

where $\xi_i = \cos \alpha_i$. The selection of the quadrature mapping is the most crucial aspect of the matrix operator approach. The constraints placed on the selection are as follows. First we must be able to properly normalize a phase function for the atmosphere due to the aerosols as in Eq. (3). Secondly we must be able to conserve the energy reflected from and transmitted through the interface. Finally we must be able to properly normalize a highly asymmetric phase function due to the hydrosol scattering in the ocean. Our solution to this problem has been enormously successful and it proceeds as follows. We first consider a Gaussian quadrature of order M for the atmosphere which is mapped into the half-space i.e., $0 < \xi \leq 1$ and of course $0 \leq \phi \leq 2\pi$. The order of the quadrature used is determined by

the condition that it must be sufficient to normalize the aerosol phase function to within 0.1%. To handle the second condition, consider a radiance stream $I(\alpha,\phi)$ striking the interface at some angle α and entering the ocean at the refracted angle θ. For the case of a continuum of radiation $I(\alpha,\phi)$ striking the interface from above, the radiance just below the interface is given by

$$I(\theta,\phi) = I(\alpha,\phi)\, t(\alpha)\, \frac{\xi\, d\xi\, d\phi}{\mu\, d\mu\, d\phi} \tag{10}$$

where $t(\alpha) = 1 - r(\alpha)$ and $r(\alpha)$ is the Fresnel reflection coefficient for unpolarized radiation given by

$$r(\alpha) = [\tan^2(\alpha-\theta)/\tan^2(\alpha+\theta) + \sin^2(\alpha-\theta)/\sin^2(\alpha+\theta)]/2 \tag{11}$$

This result holds for oblique incidence, i.e. $\alpha \neq 0$. For normal incidence Eq. (11) reduces to

$$r(0) = \left(\frac{n-1}{n+1}\right)^2 \tag{12}$$

Using Eq. (8), Eq. (10) can be written as

$$I(\theta,\phi) = I(\alpha,\phi)\, t(\alpha)\, n^2 \tag{13}$$

a result first noted by Gershun[2]. Now in the discrete approximation Eq. (10) becomes

$$I(\theta_i,\phi) = I(\alpha_i,\phi)\, t(\alpha_i)\, \frac{\xi_i}{\mu_i}\, \frac{C_i^A}{C_i^0} \tag{14}$$

where C_i^A and C_i^0 are the weights for the atmosphere and ocean respectively associated with the quadrature integration. Comparing Eq. (14) with Eq. (13) we can now determine the ocean weights C_i^0 uniquely, namely

$$C_i^0 = \frac{\xi_i C_i^A}{\mu_i n^2} . \tag{15}$$

Now $\mu_i = (1 - (1 - \xi_i^2)/n^2)^{1/2}$ where $0 < \xi_i \leq 1$ and $\mu_c < \mu_i \leq 1$ where $\mu_c = (1 - 1/n^2)^{1/2}$. The function ξ/μ is shown in Fig. 2b. The important aspect of this function is that it is bounded and has bounded derivatives of all orders. It is ideally suited for Gaussian quadrature integration since the error term for an nth order Gaussian quadrature is proportional to the 2nth derivative of the function. Since the phase function is decomposed in a series of Legendre polynomials, we must be able to integrate these polynomials with high accuracy with our mapped points and weights for the ocean. Let us now consider $\int_{\mu_c}^{1} \mu^k d\mu$ for the ocean; where k is an integer. In the discrete approximation this becomes

$$\sum_{i=1}^{M} \mu_i^k C_i^0 = \frac{1}{n^2} \sum_{i=1}^{M} \mu_i^{k-1} \xi_i C_i^A . \tag{16}$$

It should be noted that if k is odd then Eq. (16) shows that we are effectively integrating a polynomial of degree k in the atmosphere and this result will be exact as long as $k \leq 2m-1$. However if k is even then we no longer have a finite polynomial since the function we are integrating is proportional to $\xi[1 - (1 - \xi^2)/n^2]^{(k-1)/2}$. However this function is quite well behaved and has bounded derivatives of all orders and again Gaussian quadrature should do

quite well. We have tested these ideas using an 8th order Gaussian quadrature and for $0 \le k \le 15$ the worst error we encountered, which was for $k = 0$, was 2 parts in 10^{12}. All odd values of k were exact. Even for $k = 49$ the error was only 2 parts in 10^4. The next logical question to be asked is what errors are encountered if one uses Gaussian points within the critical angle for the ocean and maps them into the atmosphere? This was the technique used by Tanaka and Nakajima[3]. We will now show why this method has serious defects. With this method the atmospheric weights C_i^A are determined from the ocean weights C_i^0 by

$$C_i^A = \frac{\mu_i n^2}{\xi_i} C_i^0 \tag{17}$$

where the ocean weights are determined by using Gaussian quadrature mapped into the region $\mu_c < \mu \le 1$. If we again consider $\int_0^1 \xi^k d\xi$ then in the discrete approximation we get

$$\sum_{i=1}^{M} \xi_i^k C_i^A = \sum_{i=1}^{M} \xi_i^{k-1} \mu_i C_i^0 \tag{18}$$

For $k = 0$ we show a plot of the function μ/ξ as a function of μ in Fig. 2a. Not only is the function unbounded at $\mu = \mu_c$ but it has unbounded derivatives at this point and therefore quadrature integration should produce large errors. In general one will be integrating $\mu[1 - n^2(1 - \mu^2)]^{(k-1)/2}$ which should be exact for odd values of k up to 2m-1. However for $k = 2$ the function becomes bounded but it still has unbounded derivatives and quadrature will produce relatively large errors. For even values of $k > 2$ the function is bounded and has bounded derivatives. We tested this scheme with an 8th order Gaussian quadrature. For $k = 0$ the error was 4.6% and for $k = 2$ it was 1 part in 10^5 and becomes

better for higher values of k(even). The error for k = 49 was of the same order as the earlier method described, namely 2 parts in 10^4. It should now be clear that this latter method would be particularly bad if one is considering Rayleigh scattering for the atmosphere which is the dominant mode of scattering for the earth's atmosphere in the visual region of the spectrum.

MATRIX OPERATOR CONSTRUCTION

We will now show how to construct the appropriate matrices from the operators associated with the atmosphere, ocean, and interface. Throughout the sequel we will only consider azimuthally averaged quantities which involve only the first term in the Fourier decomposition of the phase function (see Plass, et.al.[1]). The extension to the complete decomposition is straightforward. Let $K^A(\xi_i,\xi_j) = R^A_{ij} = \underset{\sim}{R}^A$ be the matrix representation of the reflection operator R^A for the atmosphere for radiation incident on top of the layer. This matrix has dimension MxM where M is the order of quadrature for the atmosphere. Similarly $\underset{\sim}{T}^A$ is the matrix associated with the transmission operator for the layer. It also has dimensions MxM. For the ocean without the interface we have the corresponding matrices $R^0(\mu_i,\mu_j) = R^0_{ij} = \underset{\sim}{R}^0$ and $T^0(\mu_i,\mu_j) = T^0_{ij} = \underset{\sim}{T}^0$ of dimensions NxN. The reflection matrix R_{AW} going from air to water is diagonal and simply consists of the Fresnel reflection coefficients defined by Eq. (10). Similarly the transmission matrix from air to water $\underset{\sim}{T}_{AW} = \underset{\sim}{E} - \underset{\sim}{R}_{AW}$ where $\underset{\sim}{E}$ is the identity matrix and both have dimensions MxM. However to formalize our matrix products, $\underset{\sim}{T}_{AW}$ must have dimensions NxM, we must insert zeros for all elements in rows M + 1 through N. Now the reflection matrix from water to

air $\underset{\sim}{R}_{WA}$ is again diagonal and the first M elements along the diagonal are again the Fresnel reflection coefficients whereas the remaining N-M elements are all unity corresponding to total internal reflection. Similarly the transmission matrix from water to air is $\underset{\sim}{T}_{WA} = \underset{\sim}{E} - \underset{\sim}{R}_{WA}$. It should be noted that this matrix has all zero entries in rows M+1 through N. Therefore this matrix can be reduced to dimension MxN. We can now use the matrix operator formalism to set up the reflection and transmission matrices for the combined system, namely, atmosphere, interface, and ocean.

To illustrate the adding algorithm (see Plass[1], et.al.) the matrices for the combined interface and ocean are

$$\underset{\sim}{R}_{IO} = \underset{\sim}{R}_{AW} + \underset{\sim}{T}_{WA}(\underset{\sim}{E} - \underset{\sim}{R}_{O}\underset{\sim}{R}_{WA})^{-1}\ \underset{\sim}{R}_{O}\underset{\sim}{T}_{AW} \tag{19}$$

$$\underset{\sim}{T}_{IO} = \underset{\sim}{T}_{O}(\underset{\sim}{E} - \underset{\sim}{R}_{WA}\underset{\sim}{R}_{O})^{-1}\ \underset{\sim}{T}_{AW} \tag{20}$$

It should be noted that the matrix operations encountered in Eqs. (19) and (20) are at least dimensionally consistent. The matrix $\underset{\sim}{R}_{IO}$ has dimensions MxM whereas the matrix $\underset{\sim}{T}_{IO}$ has dimensions NxM. The physical interpretation of equations (19) and (20) is extremely simple if we consider writing the expression $(\underset{\sim}{E} - \underset{\sim}{R}_{O}\underset{\sim}{R}_{WA})^{-1}$ formally as a power series, namely

$$(\underset{\sim}{E} - \underset{\sim}{R}_{O}\underset{\sim}{R}_{WA})^{-1} = \underset{\sim}{E} + \underset{\sim}{R}_{O}\underset{\sim}{R}_{WA} + \underset{\sim}{R}_{O}\underset{\sim}{R}_{WA}\underset{\sim}{R}_{O}\underset{\sim}{R}_{WA} + \cdots \tag{21}$$

Therefore, using the first term in Eq. (21) and reading Eq. (19) from right to left, we see that $\underset{\sim}{T}_{AW}$ transmits the radiation through the interface, next $\underset{\sim}{R}_{O}$ reflects it from the ocean and finally $\underset{\sim}{T}_{WA}$ transmits it back through the interface and into the atmosphere. Now the second and higher order terms in

Eq. (21) simply give all orders of reflection between interface and ocean before emergence. Eq. (20) has a similar interpretation. It should also be pointed out that one can also obtain the radiation field at any interior point in the medium simply by having the reflection and transmission matrices for the medium both above and below the interior point.

PHASE FUNCTION TRUNCATION

One of the major difficulties encountered when solving the transfer equation in the ocean is the strong asymmetry in the phase function from the hydrosol scattering. To perform a normalization on such a strongly peaked function would require quadratures of extremely high order. One therefore has to consider the possibility of sacrificing some accuracy for savings in computer costs. We have adopted a technique used by Potter[4] to eleviate some of the difficulties associated with a strongly peaked phase function. The technique is basically the following. Let $P(\Theta)$ be a strongly peaked phase function subject to the normalization condition in Eq. (3). Also let $\gamma = \cos\Theta$. Now in the delta function approximation the diffraction peak is treated as a Dirac delta function and one approximates $P(\gamma)$ by

$$P(\gamma) = A\delta(1-\gamma) + P'(\gamma) \tag{22}$$

where $P'(\gamma)$ is a phase function whose diffraction peak has been removed. Using Eq. (22) and Eq. (3) we can evaluate A by

$$A = \int_{-1}^{1} [P(\gamma) - P'(\gamma)]d\gamma = \frac{1}{2\pi} - \int_{-1}^{1} P'(\gamma)d\gamma \ . \tag{23}$$

Therefore

$$\int_{-1}^{1} P'(\gamma)d\gamma = \frac{1}{2\pi} - A \ . \tag{24}$$

We can now define a properly normalized scaled phase function $P_S(\gamma)$ by

$$P_S(\gamma) = \frac{P'(\gamma)}{1 - 2\pi A} \tag{25}$$

To insure equality in the volume scattering function $\beta(\gamma)$ it is easy to see that

$$b_S = b(1 - 2\pi A) \tag{26}$$

where the subscript S is used to denote parameters involving the normalized truncated phase function. The optical depth, τ, and single scattering albedo, ω_o, transform as follows:

$$\tau_S = (b_S + a)\tau/(b + a) \tag{27}$$

$$\omega_{oS} = \omega_o(1 - 2\pi A)/(1 - 2\pi A\omega_o) \tag{28}$$

This method has been tested by Potter[4] and he found that for solar incidence angles <84° the irradiances were accurate to within 1%. A comparison between azimuthally averaged radiances for the reflected radiation agreed to within 1% for angles <87°. The transmitted radiance was also accurate to the same order except in the region of the incident beam and for small optical thicknesses. Once the optical thickness is large enough for sufficient photon diffusion, the larger discrepancies disappear.

COMPUTATIONAL RESULTS

To demonstrate the power and versatility of the matrix operator method we have considered a model whose total optical thickness $\tau_{max} = 1000$. We also assume conservative ($\omega_o = 1.0$), Rayleigh scattering throughout the region. To explore the effects due only to an interface we have placed the interface at various optical thicknesses within this region. The interface is assumed to have a refractive index of 1.338 characteristic of ocean water at visual wavelengths. The following optical quantities are computed at many points both above and below the interface and we will use the subscripts U and D to denote upwelling and downwelling radiation respectively.

$$I^o(\mu)(\text{azimuthally averaged radiance}) = \int_o^{2\pi} I(\mu,\phi)d\phi \tag{29}$$

$$H_{U,D}(\text{upward or downward irradiance}) = \int_o^1 I^o_{U,D}(\mu)\mu d\mu \tag{30}$$

$$h_{U,D}(\text{upward or downward scalar irradiance}) = \int_o^1 I^o_{U,D}(\mu)d\mu \tag{31}$$

There are other quantities derivable from these which have important physical meaning. The quantity $d(H_D - H_U)/d\tau = (1 - \omega_o)(h_D + h_U)$ is proportional to the heating rate in the medium. Also if the medium is conservative ($\omega_o = 1.0$) then $H_D - H_U$ is a constant at all depths and this is a good test

of numerical stability for an algorithm used to solve the equation of transfer. The quantity $h_D + h_U$ is proportional to the energy density in the medium. The ratio of h_D/H_D or h_U/H_U gives an indication of the degree of anistropy of the radiation field and is always greater than or equal to unity. This result is obvious from Eqs. (30) and (31). If the radiation field is isotropic then h_U/H_U or $h_D/H_D = 2.0$. If the field is highly peaked in a certain direction say μ' then h_U/H_U or $h_D/H_D \sim 1/\mu'$.

In Table 1 we present various optical quantities as a function of optical depth for a medium of optical thickness $\tau_{max} = 1000$ with conservative Rayleigh scattering throughout. No interface exists in this medium. Three solar incident angles are considered namely $\xi_o = 0.980$, 0.592, and 0.0199 corresponding respectively to solar zenith angles of $\alpha = 11.5°$, 53.7°, 88.9°. The first thing to note is that $H_D - H_U$ is constant for each ξ_o and for all optical depths and represents the downward irradiance exiting the bottom of the medium. We have also assumed a perfectly absorbing bottom. An extremely important aspect to these calculations can be observed in the irradiances H_U and H_D. In the vicinity $\tau = 10.0$ for $\xi_o = 0.980$ both H_U and H_D exceed their values at $\tau = 0$ by more than 20%, however for $\xi_o = 0.592$ a very weak maximum is reached in the vicinity of $\tau = 0.1$ whereas for $\xi_o = 0.0199$ we found no maximum. This irradiance increase is a purely three dimensional effect and does not occur in one dimension. A detailed study of this phenomenon will appear in a future publication. The ratio h_D/H_D at $\tau = 0$ is simply $1/\xi_o$, since the input is monodirectional, but by $\tau = 10$ sufficient diffusion has taken place so that the internal radiation field is quite isotropic and therefore $h_D/H_D = 2.0$. The quantity h_U/H_U at $\tau = 0$ shows significant departure from an isotropic distribution, however, at $\tau = 10$ it shows the same isotropic behavior as

the downward radiance. The reason for this is that at the top of the layer there is always a significant component of the radiance due to single scattering which of course for Rayleigh scattering is anisotropic. Once we get deep into the medium, enough scatterings have occurred that photons lose memory of their direction of entrance and thus take on an isotropic character.

In Table 2 we considered the case where a dielectric interface of refractive index 1.338 is placed at $\tau_I = 0.01$ from the top of the medium of total optical thickness $\tau_{max} = 1000$. The first thing to note is that both H_U and H_D increase by roughly a factor of two across the interface with the exception of $\xi_o = 0.0199$. The reason for this anomaly is that the direct beam is the major contributer to the downward irradiance just above the interface and at this low sun angle most of the radiation is specularly reflected upwards rather than being transmitted through the interface. For the higher sun angles a substantial part of the direct radiation is transmitted through the interface. Another factor to be considered is that the upwelling radiation beneath the interface, which lies outside the acceptance cone, gets internally reflected and therefore the interface, in a sense, acts like a trap which only allows a certain portion of the upwelling radiation to escape while the remainder gets continually recycled. Another interesting feature of this case is that h_U/H_U at $\tau = 0$ and just above the interface shows significant departure from the case where no interface is present. This is due to the fact that we are now getting a significant specular component in the upwelling radiation which tends to drive this ratio more towards $1/\xi_o$. Also by the time $\tau = 10$ is reached the radiation field becomes isotropic once again; however the irradiances still maintain higher values at equivalent

optical depths compared to the case where there is no interface.

In Table 3 we present results for the case where the interface is moved to $\tau_I = 0.1$. For this case H_U and H_D again increase across the interface for all values of ξ_o. The anomaly now disappears for low sun angles since the major contribution to the downward irradiance just above the interface is due to the diffuse component and not the direct beam, resulting in more radiation transmitted through the interface. It should also be noted that ratios of quantities are basically the same at corresponding optical depths below the interface regardless of their position.

In Table 4 the interface has been moved to $\tau_I = 10.0$. At this optical depth the effect of the interface can not be seen at the top of the medium since all the computed quantities are essentially the same compared to the case where no interface is present. Again we note the irradiance increase across the interface for all values of ξ_o and then the monotonic decrease as we move to larger optical depths.

As an additional aid to understanding the results just discussed, we can consider Figs. 3-5. Here we have plotted the diffuse component of the azimuthally averaged radiance i.e., all radiation which has undergone at least one scattering, for the case where the interface has been placed at $\tau_I = 0.01$. In Fig. 3a we show the upward diffuse component of radiance as a function of μ for various optical depths. The results have been normalized to the maximum value of the radiance at each optical depth. We first note that both at the top and just above the interface the upward diffuse radiance is darkened towards the horizon but as we cross the interface its character changes markedly. Now as we move deeper into the medium where single scattering effects become negligible the radiation field becomes isotropic. In Fig. 3b we show the diffuse downward radiance for

the same ξ_o. Just above the interface the radiance is highly peaked near the horizon. To visualize the contribution at an interior point one must realize that for the downward radiance there are two components to consider. First there is transmission of the external source through the layer above the detector and then there is reflection of the upwelling radiance from the same layer above the detector. Similar reasoning also applies to the upward radiance at an interior point. Now as we cross the interface the largest contribution to the downward radiance is coming from the radiation traveling upward below the interface. Therefore for $0 < \mu < \mu_c$ the upwelling radiance is totally internally reflected in the downward direction whereas for $\mu_c < \mu < 1$ the upwelling radiance is modified by the reflection coefficient which is close to unity for $\mu \sim \mu_c$ but falls rapidly for $\mu > \mu_c$. Thus the rapid fall-off for $\mu > \mu_c$ is simply due to the reflectance properties of the interface. Again we notice as we move deeper into the medium this strong asymmetry gradually disappears and when we reach $\tau = 10$ the radiation field is isotropic. In Figs. 4a and 4b we give similar results for $\xi_o = 0.592$. The results are qualitatively similar to the previous case. Now in Figs. 5a and 5b we have a very low sun angle; namely $\xi_o = 0.0199$ and we see a radical change in the distribution of the radiation. The upward diffuse radiance at the top of the atmosphere is now a maximum at the horizon. This phenomenon is due primarily to two effects. First we note that the downward radiance just above the interface (Fig. 5b) is peaked near the horizon. This radiation is specularly reflected into the upward stream since the reflection coefficient is high for grazing incidence. Secondly, there is more scattered radiation reaching the detector which has never penetrated the interface due to the larger optical path lengths along the directions of incidence and emergence. Also for the detectors just beneath the interface there is less separation

in the downward radiance ratio between the horizon and zenith than for the cases of higher sun angles.

CONCLUSION

We have demonstrated that the matrix operator technique can be used to give highly accurate results for the equation of transfer when coupling an atmosphere and ocean system. The advantages of the method are as follows:

1. Results for all solar incident angles are obtained in a single computer run.
2. Any type of ocean bottom can be used provided one knows its reflection properties. If one assumes a Lambert type reflecting surface then results can be obtained for many different bottom albedos in a single computer run.
3. One can easily incorporate internal detectors where all relevant physically measurable quantities can be calculated.
4. Large numbers of inhomogenous layers can be coupled to give a completely realistic representation of the atmosphere-ocean system.
5. One can also easily obtain results, from the same computer run, for an ocean whose depth can be altered by successively placing the bottom at each internal detector location, therefore one can explore bottom effects which are relevant to coastal zones.
6. Computations are quite fast. For each case presented in the paper the computation time was approximately 30 sec on an Amdahl 470V-6.

ACKNOWLEDGMENT

The research was supported by the Office of Naval Research through contract N00014-75-C-0537.

Table 1. Computed optical quantities as a function of optical depth τ for a homogenous system of optical thickness $\tau_{max} = 1000$. Rayleigh scattering is assumed everywhere and $\omega_o = 1.0$. The input solar flux is assumed to be unity in a plane perpendicular to the incoming beam.

τ	ξ_o	H_U	H_D	$H_D - H_U$	H_U/H_D	h_U/H_U	h_D/H_D	$h_U + h_D$
0	0.980	0.978	0.980	1.63-3	0.998	1.87	1.02	2.83
0	0.592	0.591	0.592	7.42-4	0.999	2.00	1.69	2.18
0	0.0199	1.98-2*	1.99-2	1.18-5	0.999	3.28	50.4	1.06
.01	0.980	0.983	0.984	1.63-3	0.998	1.87	1.07	2.90
.01	0.592	0.592	0.592	7.42-4	0.999	2.00	1.75	2.22
.01	0.0199	1.61-2	1.61-2	1.18-5	0.999	3.00	38.8	0.675
0.1	0.980	1.01	1.01	1.63-3	0.998	1.90	1.30	3.24
0.1	0.592	0.595	0.596	7.42-4	0.999	2.01	1.96	2.36
0.1	0.0199	9.96-3	9.97-3	1.18-5	0.999	2.10	3.59	5.67-2
1.0	0.980	1.15	1.16	1.63-3	0.999	1.97	1.84	4.40
1.0	0.592	0.576	0.576	7.42-4	0.999	2.02	2.09	2.37
1.0	0.0199	8.97-3	8.99-3	1.18-5	0.999	2.01	2.06	3.65-2
10	0.980	1.21	1.21	1.63-3	0.999	2.00	2.00	4.84
10	0.592	0.551	0.552	7.42-4	0.999	2.00	2.00	2.21
10	0.0199	8.76-3	8.78-3	1.18-5	0.999	2.00	2.00	3.51-2
20	0.980	1.20	1.20	1.63-3	0.999	2.00	2.00	4.80
20	0.592	0.546	0.546	7.42-4	0.999	2.00	2.00	2.18
20	0.0199	8.68-3	8.69-3	1.18-5	0.999	2.00	2.00	3.47-2
500	0.980	0.611	0.613	1.63-3	0.997	2.00	2.00	2.45
500	0.592	0.278	0.279	7.42-4	0.997	2.00	2.00	1.11
500	0.0199	4.43-3	4.44-3	1.18-5	0.997	2.00	2.00	1.77-2

*The notation -2 indicates the power of ten to be multiplied by the preceeding number.

Table 2. Computed optical quantities as a function of τ for a medium of total optical thickness τ_{max} = 1000 with a dielectric interface at τ_I = 0.01. Rayleigh scattering is assumed both above and below the interface and ω_o = 1.0. The input solar flux is assumed to be unity in a plane perpendicular to the incoming beam.

τ	ξ_o	H_U	H_D	$H_D - H_U$	H_U/H_D	h_U/H_U	h_D/H_D	$h_U + h_D$
0	0.980	0.978	0.980	2.57-3	0.997	1.79	1.02	2.75
0	0.592	0.590	0.592	1.42-3	0.998	1.83	1.69	2.08
0	0.0199	1.98-2	1.99-2	1.60-5	0.999	19.1	50.4	1.38
0.01^{A*}	0.980	0.981	0.984	2.57-3	0.997	1.78	1.07	2.80
0.01^{A}	0.592	0.591	0.592	1.42-3	0.998	1.81	1.74	2.10
0.01^{A}	0.0199	1.81-2	1.81-2	1.60-5	0.999	31.0	35.1	1.20
0.01^{B}	0.980	1.82	1.82	2.57-3	0.999	1.98	1.88	7.03
0.01^{B}	0.592	1.09	1.09	1.42-3	0.999	2.01	2.04	4.41
0.01^{B}	0.0199	1.24-2	1.24-2	1.60-5	0.999	2.01	2.08	5.10-2
0.1	0.980	1.83	1.83	2.57-3	0.999	1.98	1.89	7.07
0.1	0.592	1.09	1.09	1.42-3	0.999	2.01	2.04	4.40
0.1	0.0199	1.24-2	1.24-2	1.60-5	0.999	2.01	2.08	5.08-2
1.0	0.980	1.88	1.88	2.57-3	0.999	1.99	1.94	7.41
1.0	0.592	1.07	1.08	1.42-3	0.999	2.00	2.02	4.33
1.0	0.0199	1.21-2	1.21-2	1.60-5	0.999	2.01	2.03	4.90-2
10	0.980	1.91	1.91	2.57-3	0.999	2.00	2.00	7.64
10	0.592	1.05	1.06	1.42-3	0.999	2.00	2.00	4.22
10	0.0199	1.19-2	1.19-2	1.60-5	0.999	2.00	2.00	4.75-2
20	0.980	1.89	1.89	2.57-3	0.999	2.00	2.00	7.56
20	0.592	1.04	1.04	1.42-3	0.999	2.00	2.00	4.18
20	0.0199	1.17-2	1.18-2	1.60-5	0.999	2.00	2.00	4.70-2
500	0.980	0.964	0.966	2.57-3	0.997	2.00	2.00	3.86
500	0.592	0.533	0.534	1.42-3	0.997	2.00	2.00	2.13
500	0.0199	5.99-3	6.01-3	1.60-5	0.997	2.00	2.00	2.40-2

*Superscripts A and B refer to detectors placed just above and just below the interface respectively.

Table 3. Same as Table 2 except $\tau_I = 0.1$.

τ	ξ_o	H_U	H_D	$H_D - H_U$	H_U/H_D	h_U/H_U	h_D/H_D	$h_U + h_D$
0	0.980	0.977	0.980	2.60-3	0.997	1.85	1.02	2.81
0	0.592	0.590	0.592	1.41-3	0.997	1.95	1.69	2.15
0	0.0199	1.98-2	1.99-2	2.21-5	0.999	3.35	50.4	1.07
0.01	0.980	0.981	0.984	2.60-3	0.997	1.86	1.07	2.88
0.01	0.592	0.591	0.592	1.41-3	0.998	1.95	1.75	2.19
0.01	0.0199	1.61-2	1.61-2	2.21-5	0.999	3.08	3.88	0.676
0.1[A]	0.980	1.01	1.01	2.60-3	0.997	1.87	1.29	3.20
0.1[A]	0.592	0.593	0.594	1.41-3	0.998	1.93	1.95	2.30
0.1[A]	0.0199	1.01-2	1.01-2	2.21-5	0.998	2.98	3.60	6.65-2
0.1[B]	0.980	1.86	1.86	2.60-3	0.999	1.98	1.90	7.21
0.1[B]	0.592	1.08	1.08	1.41-3	0.999	2.01	2.04	4.37
0.1[B]	0.0199	1.69-2	1.69-2	2.21-5	0.999	2.01	2.04	6.84-2
1.0	0.980	1.91	1.91	2.60-3	0.999	1.99	1.95	7.52
1.0	0.592	1.07	1.07	1.41-3	0.999	2.00	2.02	4.30
1.0	0.0199	1.67-2	1.67-2	2.21-5	0.999	2.00	2.02	6.71-2
10	0.980	1.93	1.94	2.60-3	0.999	2.00	2.00	7.74
10	0.592	1.05	1.05	1.41-3	0.999	2.00	2.00	4.19
10	0.0199	1.64-2	1.64-2	2.21-5	0.999	2.00	2.00	6.56-2
20	0.980	1.91	1.92	2.60-3	0.999	2.00	2.00	7.66
20	0.592	1.03	1.04	1.41-3	0.999	2.00	2.00	4.14
20	0.0199	1.62-2	1.62-2	2.21-5	0.999	2.00	2.00	6.49-2
500	0.980	0.976	0.979	2.60-3	0.997	2.00	2.00	3.91
500	0.592	0.528	0.530	1.41-3	0.997	2.00	2.00	2.12
500	0.0199	8.27-3	8.30-3	2.21-5	0.997	2.00	2.00	3.31-5

Table 4. Same as Table 2 except τ_I = 10.0.

τ	ξ_o	H_U	H_D	$H_D - H_U$	H_U/H_D	h_U/H_U	h_D/H_D	$h_U + h_D$
0	0.980	0.977	0.980	2.89-3	0.997	1.87	1.02	2.83
0	0.592	0.590	0.592	1.32-3	0.998	2.00	1.69	2.18
0	0.0199	1.98-2	1.99-2	2.09-5	0.999	3.28	50.4	1.06
0.01	0.980	0.981	0.984	2.89-3	0.997	1.87	1.07	2.89
0.01	0.592	0.591	0.592	1.32-3	0.998	2.00	1.75	2.22
0.01	0.0199	1.61-2	1.61-2	2.09-5	0.999	3.00	38.8	0.675
0.1	0.980	1.01	1.01	2.89-3	0.997	1.90	1.30	3.24
0.1	0.592	0.595	0.596	1.32-3	0.998	2.01	1.96	2.36
0.1	0.0199	9.45-3	9.97-3	2.09-5	0.998	2.10	3.59	5.67-2
1.0	0.980	1.15	1.15	2.89-3	0.997	1.97	1.84	4.39
1.0	0.592	0.575	0.576	1.32-3	0.998	2.02	2.09	2.36
1.0	0.0199	8.96-3	8.98-3	2.09-5	0.998	2.01	2.06	3.65-2
10^A	0.980	1.20	1.20	2.89-3	0.998	2.00	2.00	4.80
10^A	0.592	0.546	0.548	1.32-3	0.998	2.00	2.00	2.19
10^A	0.0199	8.69-3	8.71-3	2.09-5	0.998	2.00	2.00	3.48-2
10^B	0.980	2.15	2.15	2.89-3	0.999	2.00	2.00	8.59
10^B	0.592	0.978	0.980	1.32-3	0.999	2.00	2.00	3.91
10^B	0.0199	1.55-2	1.56-2	2.09-5	0.999	2.00	2.00	6.22-2
20	0.980	2.13	2.13	2.89-3	0.999	2.00	2.00	8.51
20	0.592	0.968	0.970	1.32-3	0.999	2.00	2.00	3.88
20	0.0199	1.54-2	1.54-2	2.09-5	0.999	2.00	2.00	6.16-2
500	0.980	1.085	1.088	2.89-3	0.997	2.00	2.00	4.34
500	0.592	0.494	0.495	1.32-3	0.997	2.00	2.00	1.98
500	0.0199	7.85-3	7.88-3	2.09-5	0.997	2.00	2.00	3.15-2

References

1. Plass, G. N., Kattawar G. W., and Catchings T. E., "Matrix Operator Theory of Radiative Transfer 1: Rayleigh Scattering," Appl. Opt. 12, 314-329, (1973).

2. Gershun, A., "The Light Field," J. Math. and Phys. 18, 53-151, (1939).

3. Tanaka, M. and Nakajima T., "Effects of Oceanic Turbidity and Index of Refraction of Hydrosols on the Flux of Solar Radiation in the Atmosphere-Ocean System," J. Quant. Spectrosc. Radiat. Transfer 18, 93-111, (1977).

4. Potter, J., Jr., "The Delta Function Approximation in Radiative Transfer Theory," J. Atoms. Sci. 27, 943-949 (1970).

FIGURE CAPTIONS

Fig. 1. Geometric representation of angular variables used in the atmosphere-ocean system.

Fig. 2. a) Function transformation used for mapping ocean angular variables into atmospheric angular variables. b) Function transformation used to map atmospheric angular variables into ocean angular variables.

Fig. 3. a) Upward diffuse azimuthally averaged radiance I^0 versus μ for a conservative Rayleigh scattering medium of total optical thickness $\tau_{max} = 1000$ with a dielectric interface at $\tau_I = 0.01$ for optical depth values of 0, 0.01^A, 0.01^B, 1.0, and 10.0. Superscripts A and B refer to detectors just above and just below the interface respectively. The solar incident angle is $\xi_0 = 0.980$ ($\alpha = 1.5°$) and the results are normalized to their maximum value at each optical depth. b) Same as a) except results are for the downward diffuse I^0.

Fig. 4. a) Same as 3a except $\xi_0 = 0.592$ ($\alpha = 53.7°$). b) Same as 3b except $\xi_0 = 0.592$ ($\alpha = 53.7°$).

Fig. 5. a) Same as 3a except $\xi_0 = 0.0199$ ($\alpha = 88.9°$). b) Same as 3b except $\xi_0 = 0.0199$ ($\alpha = 88.9°$).

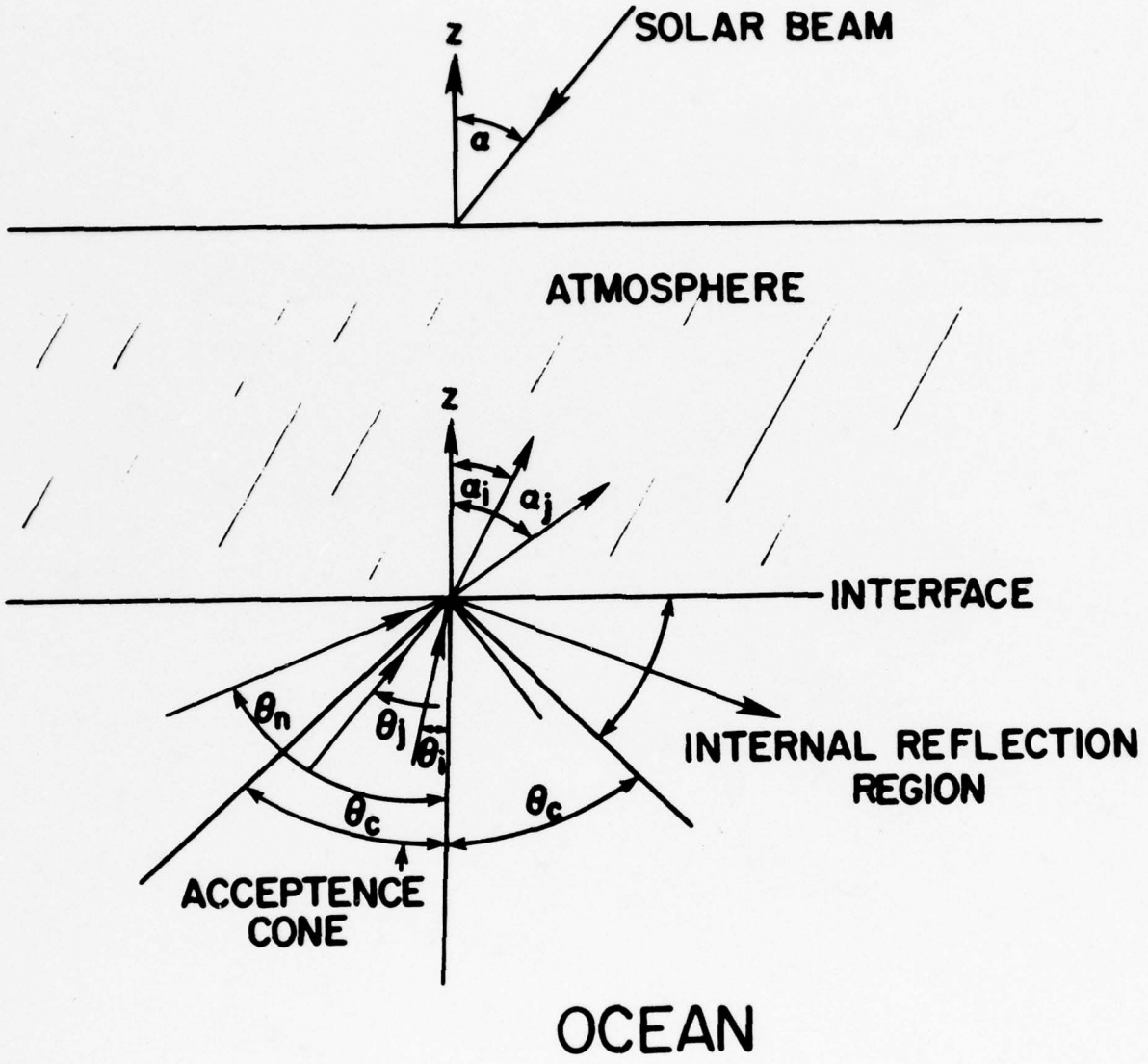
z
SOLAR BEAM
α
ATMOSPHERE
z
α_i
α_j
INTERFACE
θ_n
θ_j
$\bar{\theta}_j$
INTERNAL REFLECTION REGION
θ_c
θ_c
ACCEPTENCE CONE
OCEAN

Figure 1

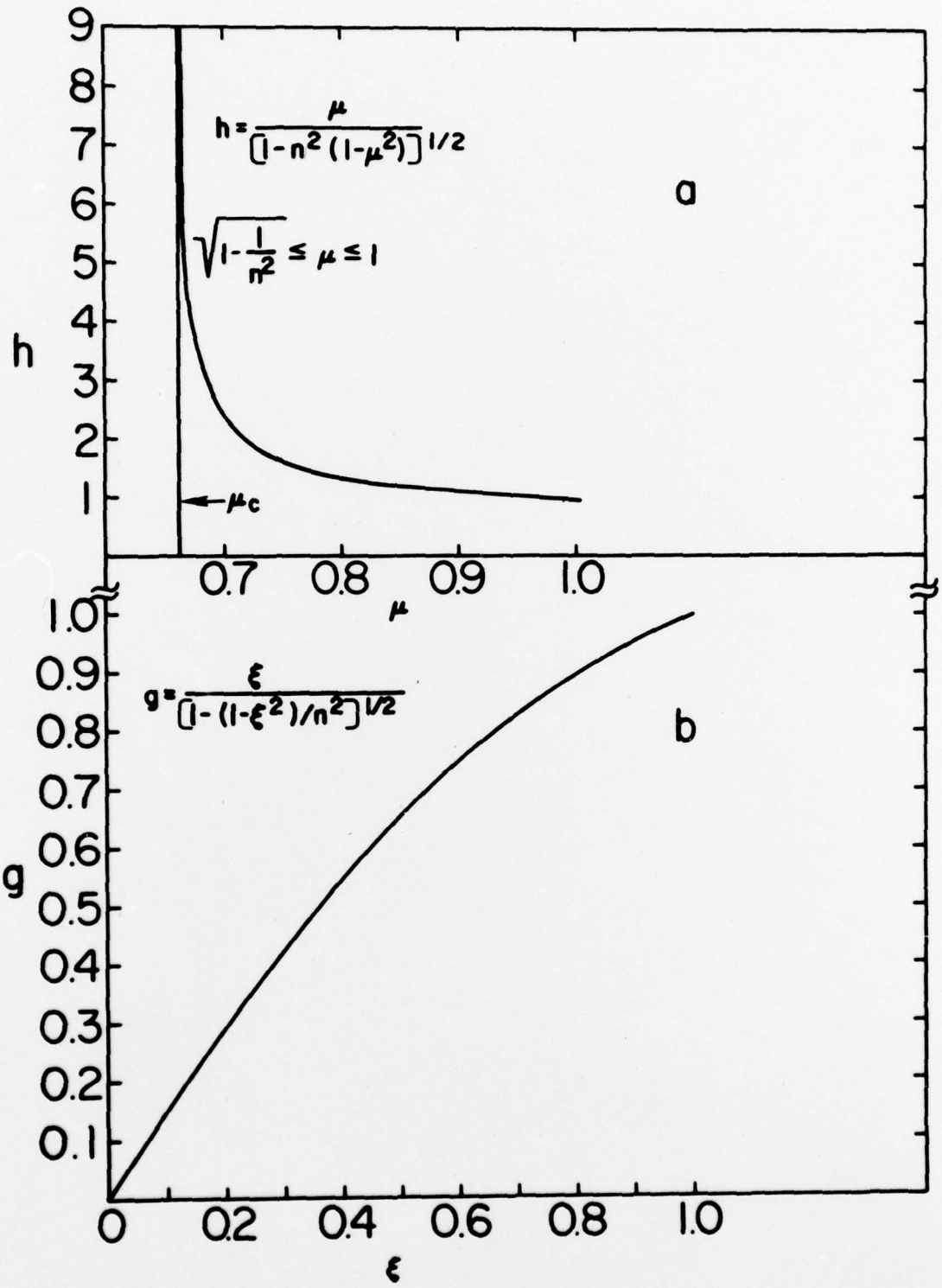

Figure 2

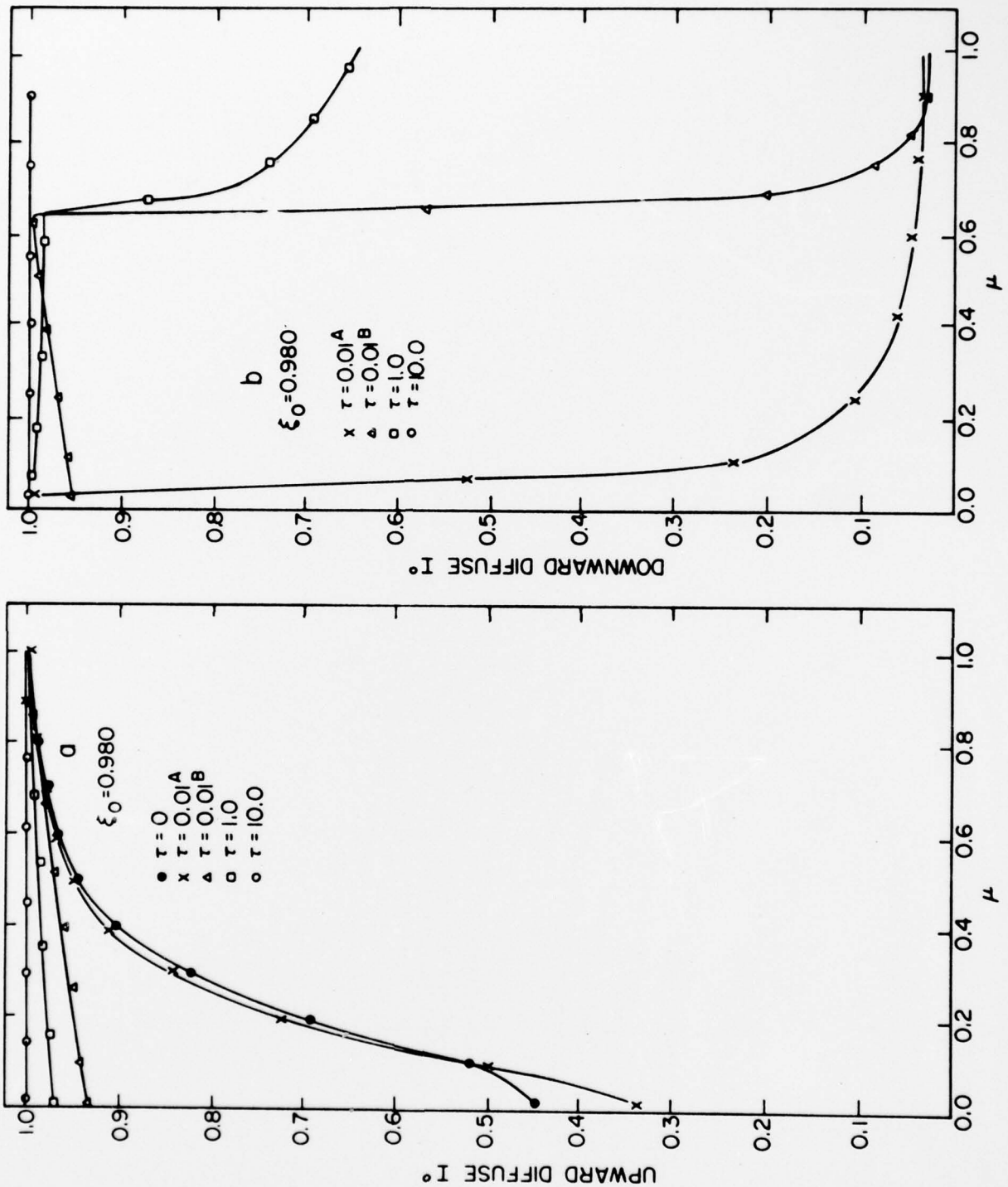
a
ξ_0=0.980
● τ = 0
× τ = 0.01^A
▲ τ = 0.01^B
□ τ = 1.0
○ τ = 10.0
UPWARD DIFFUSE I°
μ
b
ξ_0=0.980
× τ = 0.01^A
▲ τ = 0.01^B
□ τ = 1.0
○ τ = 10.0
DOWNWARD DIFFUSE I°
μ

Figure 3

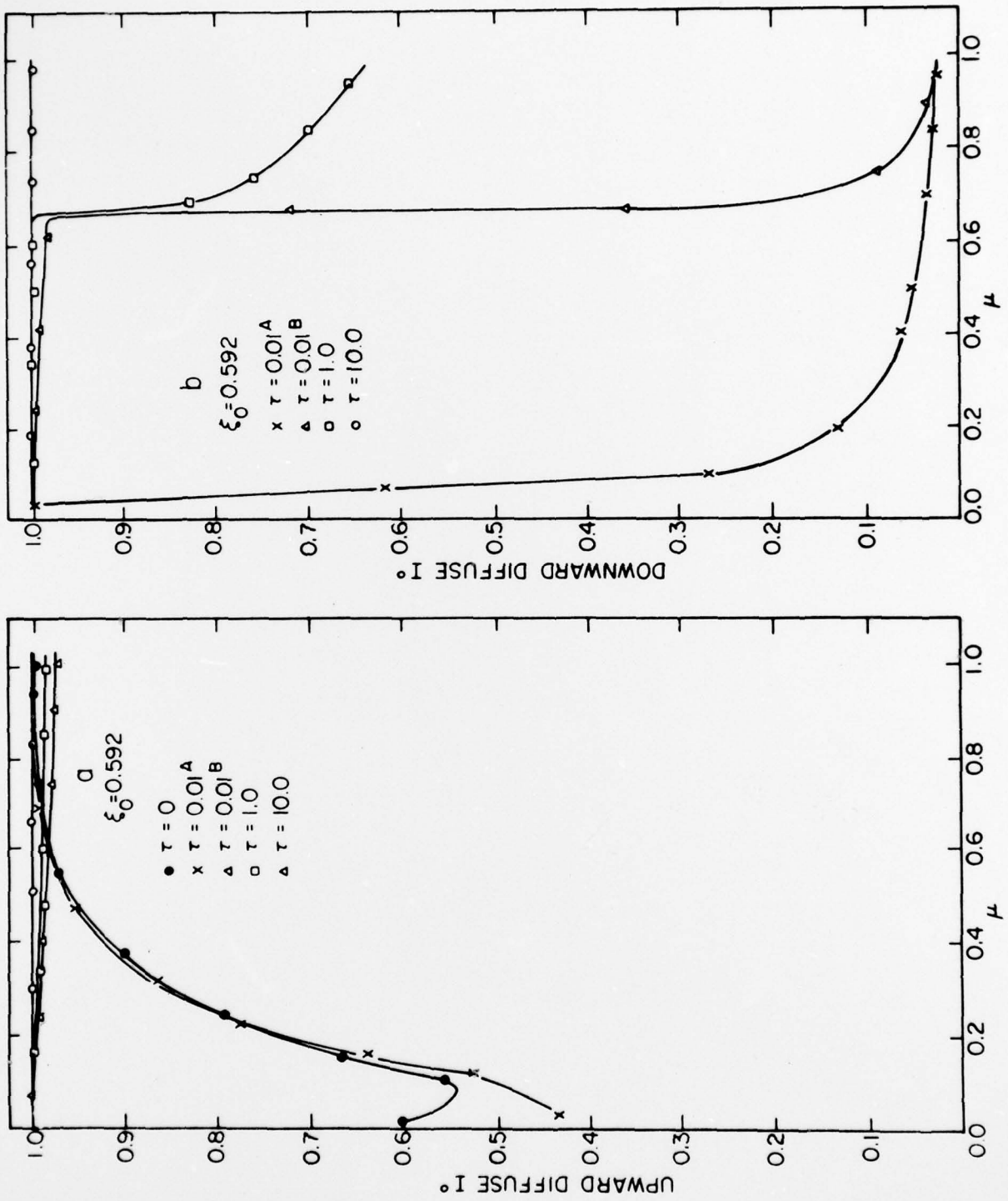
a
ξ_0=0.592
τ = 0
τ = 0.01A
τ = 0.01B
τ = 1.0
τ = 10.0
UPWARD DIFFUSE I°
μ
b
ξ_0=0.592
τ = 0.01A
τ = 0.01B
τ = 1.0
τ = 10.0
DOWNWARD DIFFUSE I°
μ

Figure 4

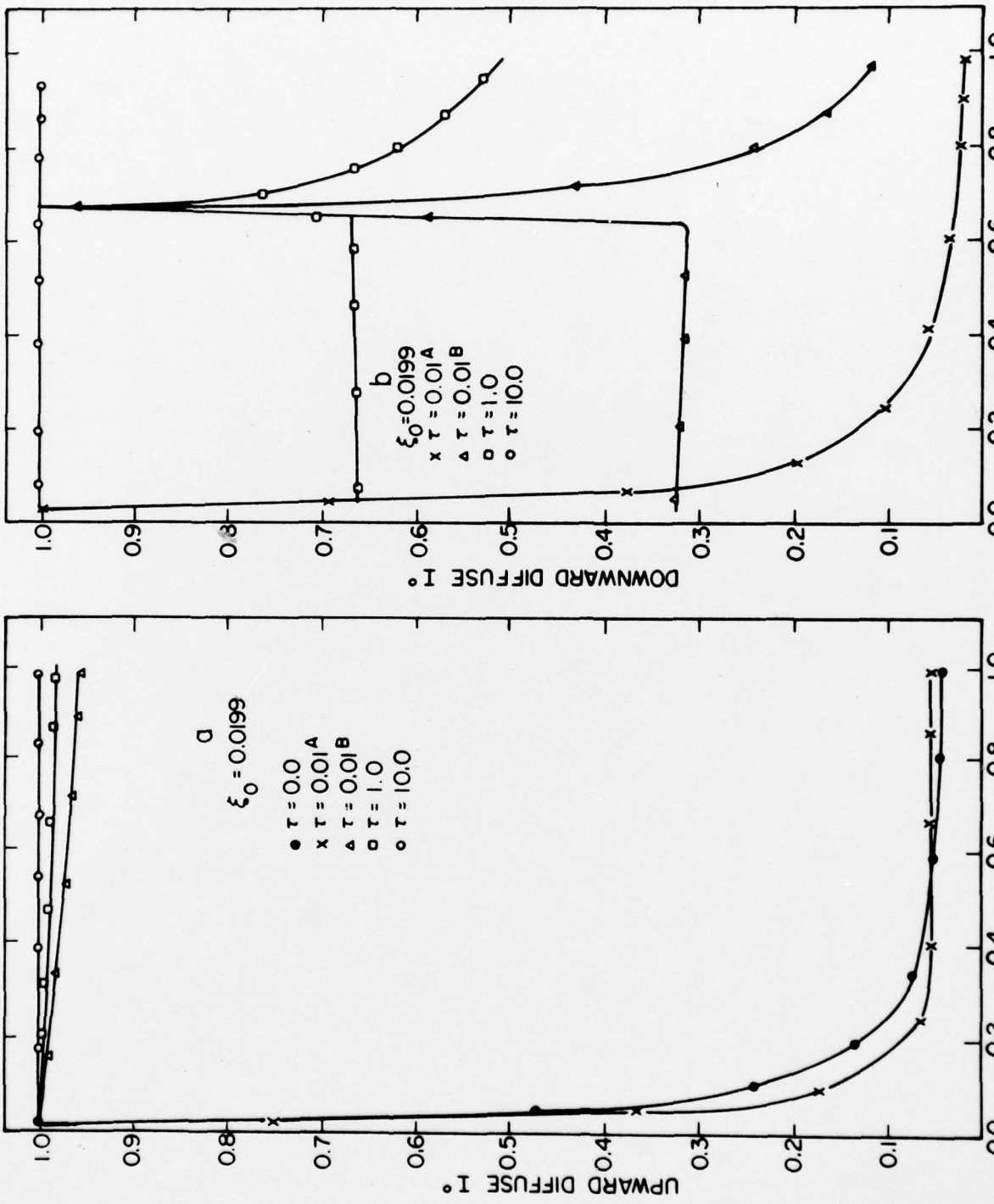
a
$\xi_0 = 0.0199$
● τ = 0.0
× τ = 0.01A
▲ τ = 0.01B
□ τ = 1.0
○ τ = 10.0
UPWARD DIFFUSE I°
μ
b
ξ_0=0.0199
× τ = 0.01A
▲ τ = 0.01B
□ τ = 1.0
○ τ = 10.0
DOWNWARD DIFFUSE I°
μ

Figure 5